Neural Network Based Modeling of a Large Steam Turbine-Generator Rotor Body Parameters From On-Line Disturbance Data

H. Bora Karayaka, Ali Keyhani, Gerald Thomas Heydt, Baj L. Agrawal, and Douglas A. Selin

***Abstract*—A novel technique to estimate and model rotor-body parameters of a large steam turbine-generator from real time disturbance data is presented. For each set of disturbance data collected at different operating conditions, the rotor body parameters of the generator are estimated using an Output Error Method (OEM). Artificial neural network (ANN) based estimators are later used to model the nonlinearities in the estimated parameters based on the generator operating conditions. The developed ANN models are then validated with measurements not used in the training procedure. The performance of estimated parameters is also validated with extensive simulations and compared against the manufacturer values.**

***Index Terms*—Artificial neural networks, large utility generators, parameter identification, rotor body parameters.**

I. Introduction

ON-LINE parameter identification for large synchronous generators is a beneficial procedure that does not require any service interruption to perform. Thus, machine parameters, which can deviate substantially from manufacturer values during on-line operation at different loading levels, can be determined without costly testing [1]. These deviations are usually due to magnetic saturation [2]–[4], internal temperature, machine aging, and the effect of centrifugal forces on winding contacts and incipient faults within the machine. The references [5]–[7] include investigations into modeling synchronous generator parameters as a function of operating condition. In most of these studies, the independent variables used in modeling nonlinear variations of the parameters are primarily the terminal voltage, current or a combination of these quantities including the phase angle. A similar study can be found in reference [7] for a small round rotor synchronous generator.

In this study, disturbance data sets acquired on-line at different loading and excitation levels of a large utility generator are utilized to identify the machine parameters. It is assumed that the machine model order is known (i.e., the number of differential equations). Estimated rotor body parameters for each operating point are then mapped into operating condition dependent machine variables using artificial neural networks. The ANN can easily identify the shape of the nonlinear function from training data. Therefore, no a prior knowledge of the shape of the mapping is required. The effects of generator saturation, rotor position and loading are included in the mapping process. Finally, extensive validation studies are conducted to investigate the performance of ANN models and estimated parameters.

Manuscript received February 25, 2000. This work was supported in part by the National Science Foundation, Grant ECS9722844.

H. B. Karayaka and A. Keyhani are with The Ohio State University, Columbus, OH.

G. T. Heydt is with Arizona State University, Tempe, AZ.

B. L. Agrawal and D. A. Selin are with the Arizona Public Service Company, Phoenix, AZ.

Publisher Item Identifier S 0885-8969(01)10053-7.

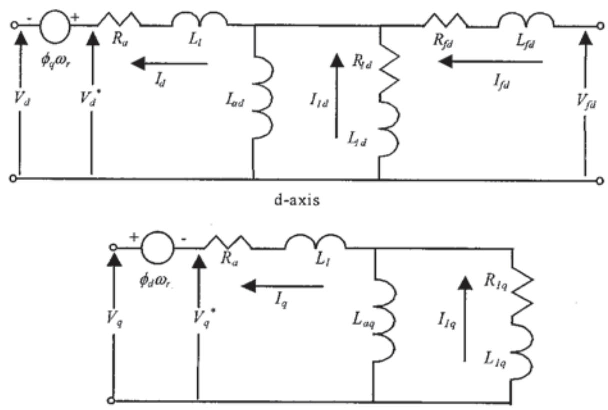

Fig. 1. On-line model structure.

II. Machine Model Description and Problem Formulation

The structure of the synchronous machine model used in this study is a *model 2.1.* type [1], with one damper in the *d-axis* and one damper in the *q-axis*, given in Fig. 1.

For continuous time systems, the state space representation of this model is,

$$dX(t)/dt = A(\theta)\cdot X(t) + B(\theta)\cdot U(t) + w(t)$$
$$Y(t) = C\cdot X(t) + v(t) \tag{1}$$

where $w(t)$ and $v(t)$ represent the process and measurement noise. Also,

$$X = [i_q\ \ i_d\ \ i_{1q}\ \ i_{1d}\ \ i^*_{fd}]^T$$
$$U = [v_q\ v_d\ \ v^*_{fd}]^T$$
$$Y = [i_q\ \ i_d\ \ i^*_{fd}]^T$$
$$\theta = [R_a\ \ R^*_{fd}\ \ R_{1d}\ \ L_l\ \ L_{ad}\ \ L_{fd}\ \ L_{1d}\ \ a\ \ R_{1q}\ \ L_{aq}\ \ L_{1q}]^T.$$

All parameters are in actual units. Also, it is assumed that the machine power angle δ is available for measurement. Variables v_d, v_q, i_d, i_q represent generator d- and q-*axis* terminal voltages and currents, respectively. The quantities i_{fd}^* and v_{fd}^* represent field current and field voltage, respectively, as measured on the field side of the generator and R_{fd}^* is the field winding resistance as measured on the field side. Terms i_{fd}, v_{fd} and R_{fd} represent corresponding transformed quantities on the stator side through the field to stator turns ratio $a = N_{fd}/N_s$ as follows,

$$i_{fd} = \frac{2}{3} a i_{fd}^* \quad v_{fd} = \frac{v_{fd}^*}{a} \quad R_{fd} = \frac{3}{2}\frac{1}{a^2} R_{fd}^*.$$

All other variables and parameters are referred to the stator.

The identification of machine parameters including armature, field and rotor body parameters involve the following five stages:

1) Measurement data is validated.
2) Using small excitation disturbance data, armature circuit parameters including field to stator turns ratio a are estimated and ANN models for saturated mutual inductances are developed.
3) Using the armature circuit parameter estimates from previous step, rotor body parameters are estimated from disturbance data acquired when the machine is operating on-line under various test conditions.
4) ANN models are developed and validated to map variables representative of generator operating condition to each rotor body parameter.
5) Estimated parameters are validated with extensive simulations in which the machine power angle δ is calculated.

Stages 1 and 2 are discussed in detail in a recent study by the authors [17]. Stages 3, 4 and 5 comprise the primary objectives of this paper.

In order to validate the established model based on estimated parameters, simulation studies are also performed and the results are compared against the simulation results with manufacturer parameters. In these studies, measured terminal and field voltages are used to excite the machine model to obtain power angle, terminal and field currents. The simulated currents and rotor angle are compared against corresponding actual measurements.

III. Measurement Configuration

The Arizona Public Service Co. (APS) Four Corners Unit 5 power generation system (including the HP and LP units) and its instrumentation are given by Fig. 2. In Fig. 2, PT1, PT2 represent the voltage measurement transformers; CT1, CT2 are current transformers; B1, B2 and B3 are circuit breakers; RCC represents the reactive current compensators; DFR represents digital fault recorder inputs; Ex is the exciter system for both the HP and LP units, rev represents the revolution of rotation of the HP units shaft; and GSU is a step up transformer (22/500 kV). The large steam turbine-generator used for study purposes was the HP Unit rated at 483 MVA, 22 kV and 3600 rpm. This unit is a participant owned unit that is operated by APS. The LP unit is not included in this study.

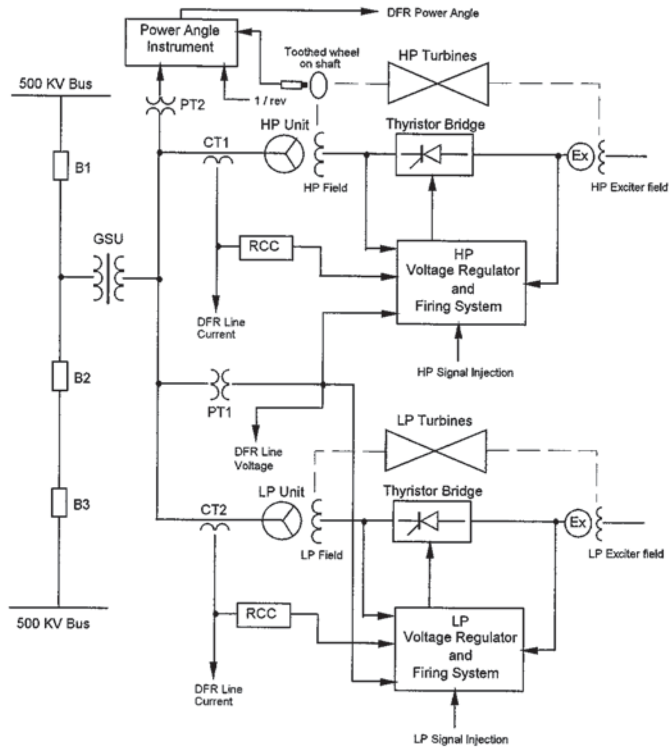

Fig. 2. Measurement setup for 4 Corners Unit 5 system.

IV. Estimation of Rotor Body Parameters

The estimation procedure involves the identification of field winding, d- and q-axis damper winding parameters from disturbance data. For estimation of rotor body parameters, operating data due to disturbances that will excite adequate amount of damper winding currents are needed. For instance, this can be achieved by perturbing the field excitation voltage in the range of five to ten percent or by capturing line fault events.

The armature circuit parameters obtained in Stage 2 [17] are fixed in this estimation procedure. These parameters include R_a, L_l, L_{ad}, L_{aq} and a. Then the parameter vector to be estimated for d-*axis* is $\theta_d = [R_{fd}^* \; L_{fd} \; R_{1d} \; L_{1d}]$ and for q-*axis* is $\theta_q = [R_{1q} \; L_{1q}]$. The model for estimation should first be established. Normally, d- and q-axis models are coupled by the speed voltage terms, $\phi_q\omega_r$ and $\phi_d\omega_r$, as can be seen in Fig. 1. In order to decouple the model, the voltages v_d^* and v_q^* should be computed as follows. The stator voltages in rotor reference frame are,

$$v_d = -R_a i_d - \phi_q \omega_r + p\phi_d \tag{2}$$

$$v_q = -R_a i_q - \phi_d \omega_r + p\phi_q. \tag{3}$$

From (2) and (3) flux dynamics are established as,

$$p\begin{bmatrix}\phi_d\\ \phi_q\end{bmatrix} = \begin{bmatrix}0 & \omega_r\\ -\omega_r & 0\end{bmatrix}\begin{bmatrix}\phi_d\\ \phi_q\end{bmatrix} + \begin{bmatrix}v_d + R_a i_d\\ v_q + R_a i_q\end{bmatrix}. \tag{4}$$

Once the flux terms are computed using (4), the voltages v_d^* and v_q^* can be found as,

$$v_d^* = v_d + \phi_q \omega_r \tag{5}$$
$$v_q^* = v_q - \phi_d \omega_r. \tag{6}$$

Finally, based on v_d^*, the decoupled d-axis and q-axis dynamics are,

$$\begin{bmatrix} v_d^* \\ v_{fd} \\ 0 \end{bmatrix} = \begin{bmatrix} -R_a & 0 & 0 \\ 0 & R_{fd} & 0 \\ 0 & 0 & R_{1d} \end{bmatrix} \begin{bmatrix} i_d \\ i_{fd} \\ i_{1d} \end{bmatrix} + \begin{bmatrix} -(L_l+L_{ad}) & aL_{ad}/1.5 & L_{ad} \\ -aL_{ad} & a^2(L_{fd}+L_{ad})/1.5 & aL_{ad} \\ -L_{ad} & aL_{ad}/1.5 & L_{1d}+L_{ad} \end{bmatrix} \cdot p \begin{bmatrix} i_d \\ i_{fd} \\ i_{1d} \end{bmatrix} \tag{7}$$

$$\begin{bmatrix} v_q^* \\ 0 \end{bmatrix} = \begin{bmatrix} -R_a & 0 \\ 0 & R_{1q} \end{bmatrix} \begin{bmatrix} i_q \\ i_{1q} \end{bmatrix} + \begin{bmatrix} -(L_l+L_{aq}) & -L_{aq} \\ -L_{aq} & -(L_l+L_{1q}) \end{bmatrix} p \begin{bmatrix} i_q \\ i_{1q} \end{bmatrix}. \tag{8}$$

The model (7)–(8) is not in the proper form for estimation. To render them amenable for state space representation, they should be rearranged. This is accomplished by taking current vector i as outputs and voltage vector v as inputs of the system, then the state space form for both models is,

$$\dot{i} = -L^{-1}Ri + L^{-1}v. \tag{9}$$

In (7) and (8), i_{1d} and i_{1q} represent unmeasurable rotor body currents for both d- and q-axis. Once the state space estimation models in the form of (7) are obtained, Output-Error-Method (OEM) can be employed for the estimation of d- and q-axis rotor body parameters. The OEM uses a block of input and output data over a fixed time period and minimizes the cost function proportional to the error between the measured and calculated outputs. In this case, the input data vector is v comprising measured field and stator voltages and the output vector is i comprising measured stator and field currents. The estimation algorithm also requires initial values for the parameters to be estimated. Manufacturer's values are utilized for this purpose.

In this study, disturbance data was collected at different operating and loading conditions by perturbing the field excitation of the machine. This was achieved by injecting step inputs into the automatic voltage regulator of the generator. A total of such ten disturbance data records were captured and made available for identification. Nine of these records include proper large transient dynamics required for the estimation of d-axis parameters and only six records include proper large transient dynamics required for q-axis. Therefore, nine sets of θ_d and 6 sets of θ_q are generated through OEM estimation.

V. Neural Network Rotor Body Models

Using artificial neural networks, the variables representative of generator operating condition are mapped to each rotor body parameter being modeled. Thus, a total of six ANNs are used to model the rotor body parameters R_{fd}^*, L_{fd}, R_{1d}, L_{1d}, R_{1q}, L_{1q}.

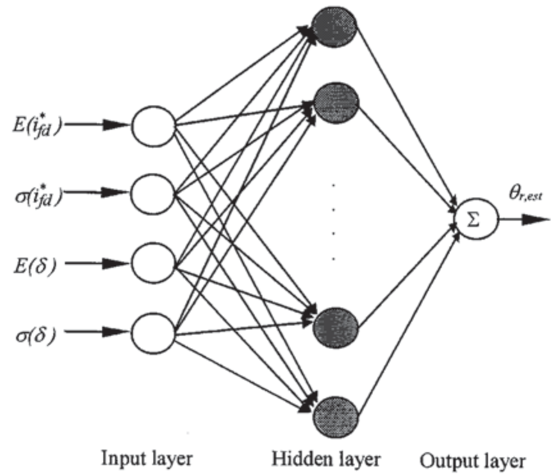

Fig. 3. Rotor body ANN model.

The generator testing procedure is generally conducted at rated terminal voltage. Hence, the operating region of the generator can be determined by using the field current i_{fd}^* and power angle δ. Due to the fact that the variables i_{fd}^* and δ are not constant during a disturbance, there is no one unique point that can represent each measurement record to be used to develop ANN models of rotor body parameters. Therefore, some statistical variables that are defined based on i_{fd}^* and δ are used in this study to represent each operating point defined by a specific disturbance data set. Well-known statistical variables, mean value and standard deviations of i_{fd}^* and δ (described in the Appendix) are used for this purpose. Thus, each rotor body ANN model consists of four inputs, one output and a single hidden layer having arbitrary number of processing elements to be determined by the training procedure. Mathematical formulation of this ANN model is given as,

$$\begin{aligned} P &= [E(\boldsymbol{i_{fd}^*})\ \ \sigma(\boldsymbol{i_{fd}^*})\ \ E(\delta)\ \ \sigma(\delta)]^T \\ \theta_{r,est} &= W_2 \cdot \tanh(W_1 \cdot P + B_1) + B_2 \end{aligned} \tag{10}$$

where P is the input vector. Notations E and σ refer to mean value and standard deviation, respectively. Notations $\boldsymbol{i_{fd}^*}$ and δ represent field current and power angle arrays given in each measurement record. The output of neural network $\theta_{r,est}$ refers to the rotor body parameter estimated by corresponding ANN model. $E(\boldsymbol{i_{fd}^*})$, $\sigma(\boldsymbol{i_{fd}^*})$ are computed based on per unit field current and $E(\delta)$, $\sigma(\delta)$ are in units of radians so as to keep each ANN input in the same numeric range. W_1, B_1, W_2 and B_2 are the weight and bias matrices to be adjusted to train the network. The description of these matrices can be found in [7]. The structure of this ANN is visualized in Fig. 3.

It is desirable to visualize the transfer functions of rotor body parameters with respect to all variables of input vector space P, however; this can be at most represented in three dimensions. For example, the approximate nonlinear mappings between $E(\boldsymbol{i_{fd}^*})$, $E(\delta)$ and operating condition dependent rotor body parameters are portrayed in Figs. 4–6. These 3-D plots represent the variation manifolds within the bounds of estimated parameter values.

During the weight adjustment procedure a trial and error procedure is used to determine the number of hidden layer

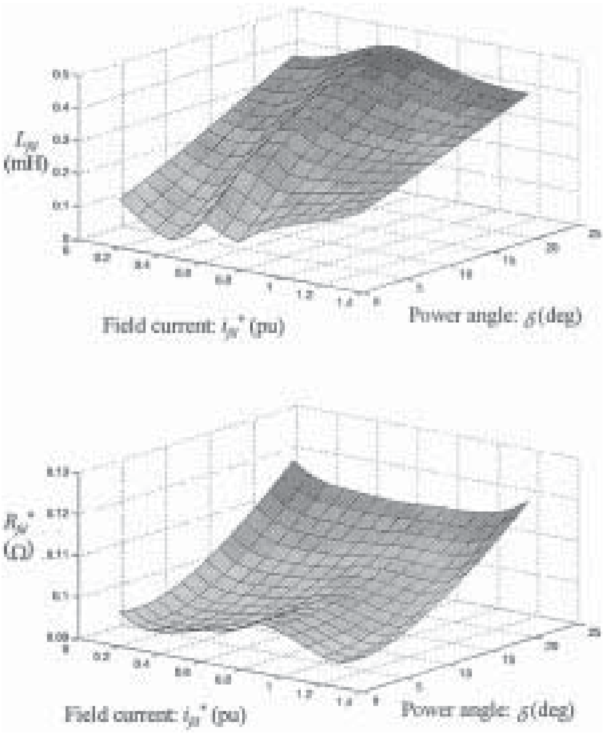

Fig. 4. Transfer functions of L_{fd} and R_{fd}^* w.r.t. the mean values of i_{fd}^* and δ.

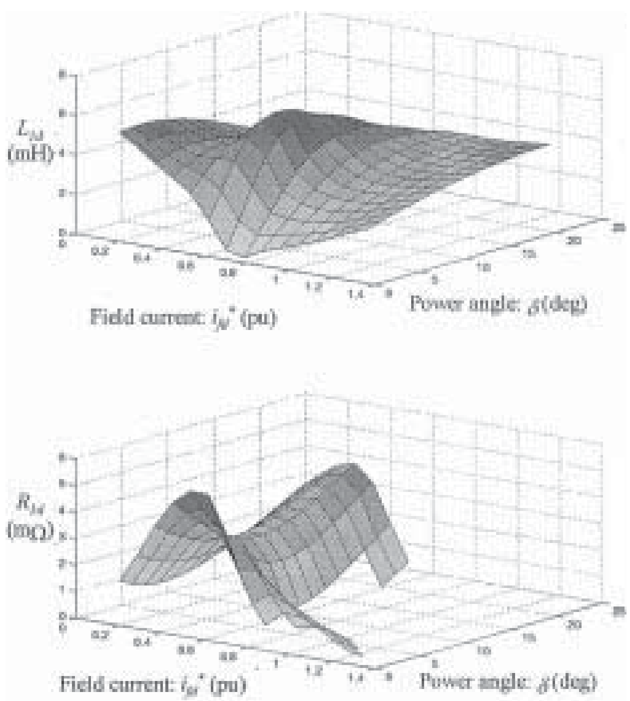

Fig. 5. Transfer functions of L_{1d} and R_{1d} w.r.t. the mean values of i_{fd}^* and δ.

neurons. A satisfactory convergence criterion has been met with five hidden layer neurons for each ANN estimator. All ANN models are trained using Levenberg–Marquardt algorithm [18]. The results of training procedure for R_{1d} and L_{1d} are given in terms of the weights and biases in the Appendix. Due to the space limitations, the weights and biases for the other parameters are not given.

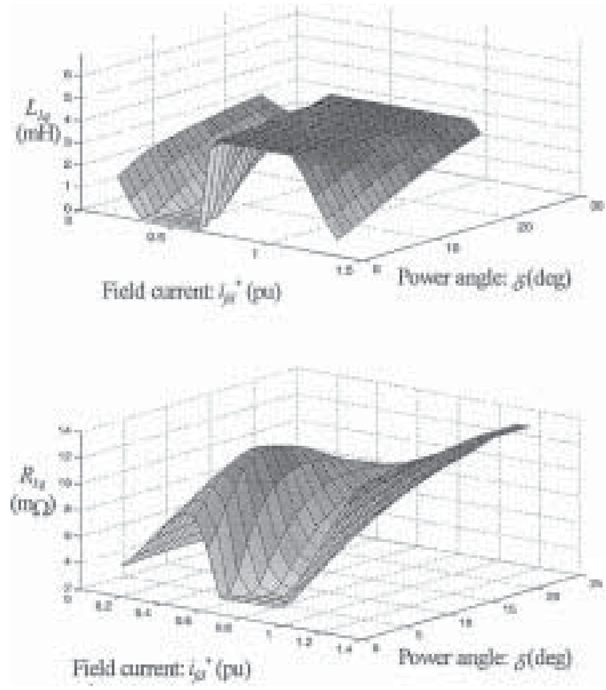

Fig. 6. Transfer functions of L_{1q} and R_{1q} with respect to the mean values of i_{fd}^* and δ.

TABLE I
COMPARISON OF OEM ESTIMATED AND ANN ESTIMATED PARAMETERS FOR THE CROSS VALIDATION DATA SET

	R_{fd}^* (Ω)	L_{fd} (mH)	R_{1d} (mΩ)	L_{1d} (mH)
OEM Estimate	.1009	.1075	2.7294	.5275
ANN Estimate	.0965	.1038	2.8100	.4544
% Error	4.36	3.44	2.87	13.8

In order to verify that the networks are able to generalize properly, a cross validation data set, which is not included in the training, is used after the training. Table I compares ANN estimated and OEM estimated d-axis parameters for the data set not used in training. As can be seen, ANN models can correctly interpolate for the patterns not used in training.

Due to the very limited number of data sets available for the q-axis rotor body parameter estimates, all estimates are used for ANN model training and not left to the validation procedure. It is expected that the more disturbance data sets are provided for this machine, the better estimates will be obtained by the rotor body ANN models for previously unseen data patterns.

VI. PARAMETER VALIDATIONS

For the purpose of comparatively validating estimated and manufacturer parameters, Four Corners HP unit are simulated for per-unit model in the time domain. Eventually, the machine output variables obtained from simulation studies are compared with the measurement records.

The simulation models are developed in Matlab programming environment. First the state space equations have to be established. The machine mathematical model includes both electrical and mechanical dynamics. The electrical dynamics

TABLE II
ERROR STATISTICS OF SIMULATED MACHINE VARIABLES FOR THE FIRST CYCLE OF THE DISTURBANCE

Simulated machine variable statistics			Test 1	Test 2	Test 3	Test 4
i_q (kA)	*Error mean*	E*	0.2058	0.1926	0.4130	0.0524
		M**	0.3101	0.2959	0.9458	0.1309
	Error variance	E	0.0435	0.0381	0.2831	0.0028
		M	0.0989	0.0900	1.0464	0.0176
i_d (kA)	*Error mean*	E.	0.0050	0.0464	0.1828	2.0715
		M	3.5531	3.6241	3.2867	5.5473
	Error variance	E	0.0000	0.0022	0.0347	4.4102
		M	12.976	13.499	11.103	31.627
i_{fd}^* (kA)	*Error mean*	E.	0.0009	0.0012	0.0215	0.3165
		M	0.5808	0.5724	0.5326	1.2216
	Error variance	E.	0.0000	0.0000	0.0005	0.1055
		M	0.3467	0.3367	0.2915	1.5339
δ (degree)	*Error mean*	E	1.3904	1.4176	0.8356	0.1495
		M	1.9436	1.9847	5.7259	14.821
	Error variance	E	1.9885	2.0683	0.7176	0.0272
		M	3.8839	4.0514	33.699	225.78

* Value obtained using estimated parameters,
** Value obtained using manufacturer' parameters,

TABLE III
ERROR STATISTICS OF SIMULATED MACHINE VARIABLES FOR THE FIRST 60 CYCLES OF THE DISTURBANCE

Simulated machine variable statistics			Test 1	Test 2	Test 3	Test 4
i_q (kA)	*Error mean*	E*	0.2023	0.1972	0.4341	1.1680
		M**	0.3063	0.3035	0.7016	1.5285
	Error variance	E	0.0411	0.0390	0.3195	1.5499
		M	0.0941	0.0923	0.7124	2.8439
i_d (kA)	*Error mean*	E.	0.0372	0.0648	0.2180	1.1350
		M	3.6682	3.7618	3.7421	3.2465
	Error variance	E	0.0017	0.0045	0.0645	1.4516
		M	13.492	14.192	14.171	11.5084
i_{fd}^* (kA)	*Error mean*	E.	0.0041	0.0078	0.0287	0.1249
		M	0.5935	0.5950	0.6239	0.7126
	Error variance	E.	0.0000	0.0001	0.0016	0.0217
		M	0.3531	0.3549	0.3912	0.5340
δ (degree)	*Error mean*	E	1.3843	1.4305	1.6282	1.4099
		M	1.9490	2.0146	4.5504	18.255
	Error variance	E	1.9213	2.0546	3.9814	3.3327
		M	3.8081	4.0716	21.316	335.01

* Value obtained using estimated parameters,
** Value obtained using manufacturer' parameters,

are given by (1) for the identification model. For the manufacturer model, the only difference is that there is one extra damper winding in the q-axis model (*model 2.2* [1]). The mechanical dynamics for both models can be given as,

$$\dot{\omega}_r = \frac{1}{2H}(T_{pm} - T_e) + B\omega_r$$
$$\dot{\delta} = \omega_r - \omega_e \tag{11}$$

where
- B damping constant;
- H inertia constant;
- T_{pm} represents prime mover torque;
- T_e represents electromagnetic torque.

For the complete state space model, the system state, input and output vectors, respectively, are given as,

$$X = [i_q \ i_d \ i_{1q} \ i_{1d} \ i_{fd}^* \ \omega_r \ \delta]^T$$
$$U = [v_t \ v_{fd}^* \ T_{pm}]^T$$
$$Y = [i_q \ i_d \ i_{fd}^* \ \delta]^T$$

where v_t represents terminal voltage peak value and can be computed in terms of line-to-line stator voltage measurements. The state vector X also includes i_{2q} for the manufacturer model. Since T_{pm} is not measured, some assumptions have to be made for T_{pm} calculations:

- For disturbances that result in small active power changes, T_{pm} is assumed to be constant and equal to the initial value of T_e.
- For disturbances that result is substantial active power changes, T_{pm} is assumed to be equal to P_{active}/ω_r by neglecting electromechanical power losses.

For the simulations, 3rd order Runge–Kutta method is utilized as the differential equation solver. For the first electrical cycle of the disturbance, the mean and variance of the simulation errors are listed in Table II for some of the measurement records. Table III lists the error statistics for the first 60 cycles of the disturbance.

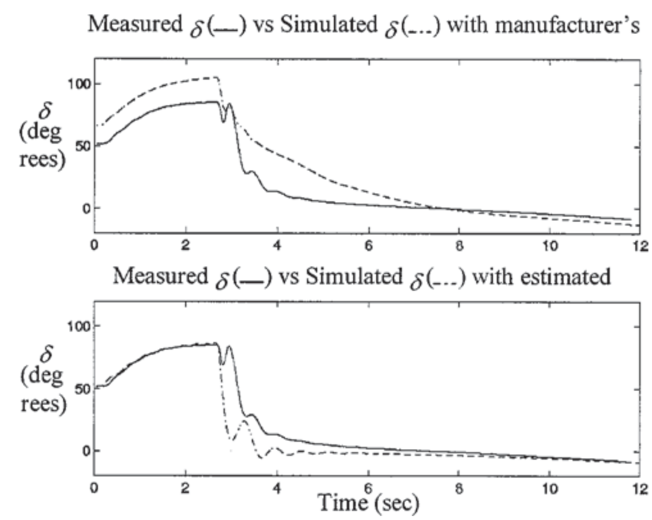

Fig. 7. The simulated δ vs. measured δ for both estimated and manufacturer parameters.

As can be seen from Tables II and III, the simulations, with estimated parameters, perform much better than simulations with manufacturer parameters. Especially for Tests 3 and 4 where the unit is tripped, the simulation errors for δ are quite substantial for manufacturer parameters. Also for Test 4, the simulated machine variables vs. measurement data records are plotted for entire data set and given by Figs. 7–10.

VII. CONCLUSION

An Artificial Neural Network based modeling technique for the rotor body parameters of a large utility generator is developed. Disturbance operating data collected on-line at different levels of excitation and loading conditions are utilized for

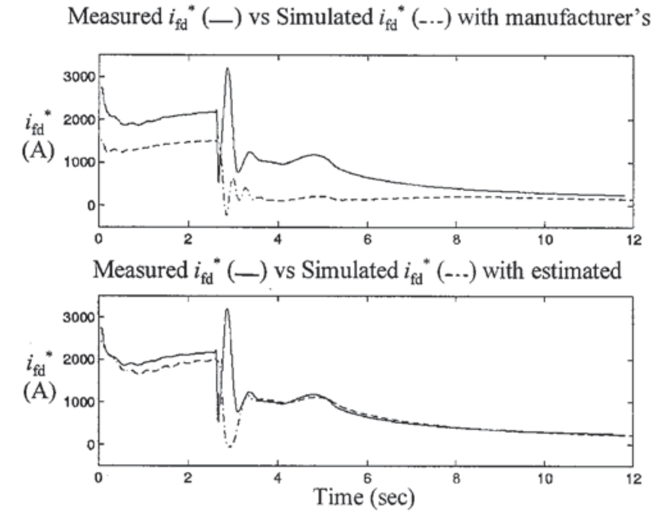

Fig. 8. The simulated i_{fd}^* vs. measured i_{fd}^* for both estimated and manufacturer parameters.

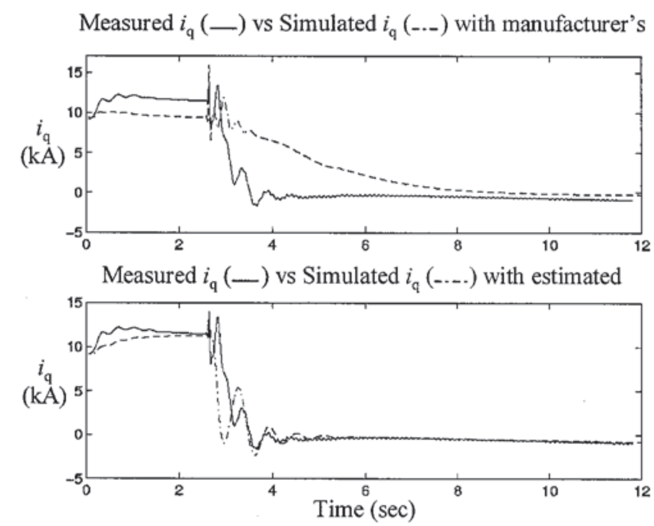

Fig. 9. The simulated i_q vs. measured i_q for both estimated and manufacturer parameters.

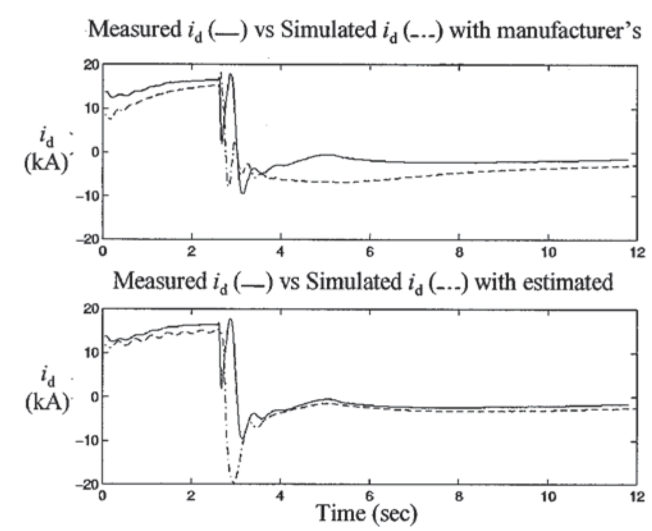

Fig. 10. The simulated i_d vs. measured i_d for both estimated and manufacturer parameters.

estimation. The disturbance data are obtained by perturbing the field side of the machine in large amounts. An OEM technique is later employed to estimate the operating point dependent rotor body parameters. Rotor body ANN models are developed by mapping field current i_{fd}^* and power angle δ to the parameter estimates.

Validation studies show that ANN models can correctly interpolate between patterns not used in training.

It is expected that richer data set collected at different loading and excitation levels would improve the performance of such ANN models. It has also been shown through extensive simulations that the estimated parameters can correctly predict the internal variables of the machine during large transient events. Only field and terminal voltage measurements are utilized during these simulations.

APPENDIX

The estimated weights and biases for L_{1d} ANN model

Input to Hidden Layer

Weights, $W1$

$$\begin{array}{rrrr} 0.9788 & 3.2250 & 1.5682 & -3.0754 \\ -2.1159 & 4.1708 & -5.1911 & -0.3545 \\ -0.3607 & 2.6550 & -5.3582 & 0.9816 \\ -0.1081 & -6.0435 & -3.2224 & -4.0616 \\ 1.0061 & -3.4998 & 2.1998 & -4.3176 \end{array}$$

Biases, $B1^T$

$$\begin{array}{rrrrr} -1.5524 & 1.2151 & 2.3107 & 0.1652 & 1.5486 \end{array}$$

Hidden Layer to Output

Weights, $W2$

$$\begin{array}{rrrrr} 1.7618 & 5.4068 & -0.9097 & -5.4107 & 2.3757 \end{array}$$

Bias, $B2$

$$1.0925$$

The estimated weights and biases for R_{1d} ANN model

Input to Hidden Layer

Weights, $W1$

$$\begin{array}{rrrr} 0.5659 & -4.6565 & -3.8250 & 0.7801 \\ -1.7650 & -0.9102 & 4.3498 & -1.6474 \\ -3.3118 & 2.7679 & 1.7180 & -2.3505 \\ -0.2118 & -3.8658 & -0.9416 & -3.2274 \\ 1.2872 & -6.7329 & -2.2611 & -3.4213 \end{array}$$

Biases, $B1^T$

$$\begin{array}{rrrrr} 0.3642 & 1.4991 & 2.4391 & 2.5116 & -0.3280 \end{array}$$

Hidden Layer to Output

Weights, $W2$

$$\begin{array}{rrrrr} 1.0870 & 3.8530 & 3.5253 & -3.2647 & 5.5263 \end{array}$$

Bias, $B2$

$$2.1265.$$

ACKNOWLEDGMENT

The authors acknowledge the assistance of J. Demcko of APS.

REFERENCES

[1] *IEEE Guide for Synchronous Generator Modeling Practices in Stability Analysis*, IEEE Std. 1110, 1991.

[2] A. El-Serafi, A. Abdallah, M. El-Sherbiny, and E. Badawy, "Experimental study of the saturation and the cross-magnetizing phenomenon in saturated synchronous machines," *IEEE Trans. Energy Conversion*, vol. EC-3, pp. 815–823, Dec. 1988.

[3] F. De Mello and L. Hannett, "Representation of saturation in synchronous machines," *IEEE Trans. Power Systems*, vol. 1, pp. 8–14, Nov. 1986.

[4] S. Minnich, R. Schulz, D. Baker, D. Sharma, R. Farmer, and J. Fish, "Saturation functions for synchronous generators from finite elements," *IEEE Trans. Energy Conversion*, vol. 2, pp. 680–687, Dec. 1987.

[5] H. Tsai, A. Keyhani, J. A. Demcko, and D. A. Selin, "Development of a neural network saturation model for synchronous generator analysis," *IEEE Trans. Energy Conversion*, vol. 10, no. 4, pp. 617–624, Dec. 1995.

[6] L. Xu, Z. Zhao, and J. Jiang, "On-line estimation of variable parameters of synchronous machines using a novel adaptive algorithm—Estimation and experimental verification," *IEEE Trans. Energy Conversion*, vol. 12, no. 3, pp. 200–210, Sept. 1997.

[7] S. Pillutla and A. Keyhani, "Neural network based modeling of round rotor synchronous generator rotor body parameters from operating data," *IEEE Trans. Energy Conversion*, vol. 14, pp. 321–327, Sept. 1999.

[8] H. Tsai, A. Keyhani, J. A. Demcko, and R. G. Farmer, "On-line synchronous machine parameter estimation from small disturbance operating data," *IEEE Trans. Energy Conversion*, vol. 10, no. 1, pp. 25–36, Mar. 1995.

[9] K. S. Narendra and K. Parthasarathy, "Identification and control of dynamical systems using neural networks," *IEEE Trans. Neural Networks*, vol. 1, pp. 4–27, 1990.

[10] I. M. Canay, "Causes of discrepancies on calculation of rotor quantities and exact equivalent diagrams of the synchronous machine," *IEEE Trans. Power Apparatus and Systems*, vol. PAS-88, no. 7, pp. 1114–1120, July 1969.

[11] J. L. Kirtley, Jr., "On turbine-generator rotor equivalent circuit structures for empirical modeling of turbine generators," *IEEE Trans. Power Systems*, vol. PWRS-9, no. 1, pp. 269–271, 1994.

[12] I. Kamwa, P. Viarouge, and J. Dickinson, "Identification of generalized models of synchronous machines from time-domain tests," *IEE Proceedings C*, vol. 138, no. 6, pp. 485–498, Nov. 1991.

[13] S. Salon, "Obtaining synchronous machine parameters from test," in *Symposium on Synchronous Machine Modeling for Power Systems Studies*. Piscataway, NJ, USA, 83THO101-6-PWR.

[14] S. R. Chaudhary, S. Ahmed-Zaid, and N. A. Demerdash, "An artificial neural network model for the identification of saturated turbo-generator parameters based on a coupled finite-element/state-space computational algorithm," *IEEE Trans. Energy Conversion*, vol. 10, pp. 625–633, Dec. 1995.

[15] J. A. Demcko and J. P. Chrysty, "Self-calibrating power angle instrument," Research Project 2591-1 Final Report, EPRI, EPRI GS-6475, vol. 2, Aug. 1989.

[16] M. A. Arjona and D. C. Macdonald, "A new lumped steady-state synchronous machine model derived from finite element analysis," *IEEE Trans. Energy Conversion*, vol. 14, no. 1, pp. 1–7, Mar. 1999.

[17] H. Karayaka, A. Keyhani, B. Agrawal, D. Selin, and G. Heydt, "Identification of armature, field and saturated parameters of a large steam turbine-generator from operating data," IEEE Trans. Energy Conversion, Preprint Order no. PE064EC (05-1999), to be published.

[18] M. Hagan and M. B. Menhaj, "Training feedforward networks with the Marquardt algorithm," *IEEE Trans. Neural Networks*, vol. 5, no. 6, pp. 989–993, Nov. 1994.

H. Bora Karayaka received the B.S.E.E. and M.S.E.E. degrees from Istanbul Technical University, Istanbul, Turkey, in 1987 and 1990, respectively. Since 1996, he has been a research associate at The Ohio State University. He is currently working toward his Ph.D. in the Department of Electrical Engineering, The Ohio State University, Columbus, OH.

Ali Keyhani received the Ph.D. degree from Purdue University, West Lafayette, IN, in 1975. Dr. Keyhani is a Professor of Electrical Engineering at the Ohio State University, Columbus, OH. His research interests are in control and modeling, parameter estimation, failure detection of electric machines, transformers and drive systems.

Gerald Thomas Heydt received the B.E.E.E. degree from the Cooper Union in New York, and the M.S.E.E. and Ph.D. degrees from Purdue University in West Lafayette, IN. He is a Professor of Electrical Engineering at Arizona State University.

Baj L. Agrawal received the B.S. degree in electrical engineering from Birla Institute of Technology and Science, India, in 1970, and the Masters and Ph.D. degrees from the University of Arizona, Tucson. Dr. Agrawal joined Arizona Public Service Company, in 1974, where he is currently working as a Senior Consulting Engineer.

Douglas A. Selin received the B.S.E.E. degree in 1983 from Brigham Young University and the M.E. degree from Rensselaer Polytechnic Institute, in 1984. In 1984, he joined Arizona Public Service Company where his responsibilities include subsynchronous resonance problem analysis and simulation of power system dynamics and transients.